(28) V. J. Minkiewicz, D. E. Cox, and G. Shirane, *Solid State Commun.*, **8**, 1001 (1970).
(29) We present here a very general and necessarily brief summary of the proposed mechanism. For detailed information the reader is referred to refs 4–17.
(30) N. Achiwa, *J. Phys. Soc. Jpn.*, **27**, 561 (1969).
(31) M. T. Hutchings, G. Shirane, R. J. Birgeneau, and S. L. Holt, *Phys. Rev. B*, **5**, 1999 (1972).

Contribution from the Wright and Rieman Chemistry Laboratories, Rutgers, The State University of New Jersey, New Brunswick, New Jersey 08903, and Bell Laboratories Murray Hill, New Jersey 07974

Resonance Raman Spectra and Electronic Structure of Binuclear μ-Oxo-Bridged Decahalo Transition Metal Complexes $M_2OX_{10}^{4-}$, M = Ru, Os, W

JOSEPH SAN FILIPPO, Jr.,*[1a] PAUL J. FAGAN,[1a] and FRANK J. DI SALVO[1b]

Received November 3, 1976 AIC60791N

Excitation profiles have been obtained for the structurally related, linear μ-oxo-bridged complexes $Ru_2OCl_{10}^{4-}$, $Ru_2OBr_{10}^{4-}$, $Os_2OCl_{10}^{4-}$, and $W_2OCl_{10}^{4-}$. They reveal that the intense, low-frequency, totally symmetric metal–oxygen–metal stretching vibration which is the dominant feature in the resonance Raman spectra of these ions is coupled to a single electronic transition involving electrons spanning the M–O–M group. These observations establish that the M–O–M unit in these complexes is an electronically unique, independent chromophore. The suggested assignment for this transition, based on the Dunitz–Orgel molecular orbital description of the π bonding in these complexes, involves the promotion of an electron from a nonbonding e_g orbital to an antibonding e_u orbital. The utility of these observations and conclusions as they relate to the electronic structure of other linear and near-linear μ-oxo-bridged complexes is discussed. In addition, a study of the magnetic susceptibility of $K_4W_2OCl_{10}$ suggests that the previous view of this material as consisting of a mixed valent ion W^{III}–O–W^{V} is incorrect, but is consistent with the view that the two tungsten centers share equivalent d^2 configurations and are antiferromagnetically coupled with an exchange energy of ~75 K. The nonzero susceptibility at low temperatures is most readily accounted for by this exchange, a significant spin–orbit coupling, and C_4 crystal field combining to produce Van Vleck coupling to an excited magnetic state.

Introduction

Early interest in linear μ-oxo-bridged transition metal complexes centered about their diamagnetism, the unusual (linear) geometry of the metal–oxygen–metal unit, and the significantly shorter than usual metal–oxygen bond distance. The initial novelty of these complexes has been gradually replaced by their near-routine acceptance as a common structural unit. The recent recognition that linear and near-linear μ-oxo-bridged transition metal complexes appear biochemically in such systems as the protein hemerythrin has provided added stimulus to the study of these complexes.[2]

We recently reported that Raman spectroscopy can provide a convenient spectroscopic technique for the detection and study of certain μ-oxo-bridged complexes.[3] In the specific examples examined viz., $M_2OX_{10}^{4-}$ (M = Ru, Os, W; X = Cl, Br), the Raman spectra were characterized by the intense, easily identifiable symmetric M–O–M stretching vibration, ν_1, with overtone progressions that extend in some instances to at least 6 ν_1 as well as a series of combination band progressions, the most outstanding of which corresponded to $n\nu_1 + \nu_2$ [$\nu_2 = \nu(M\text{–}X_{terminal})$] and $n\nu_1 + \nu_5$ [$\nu_5 = \nu(M\text{–}X_{radical})$]. As part of our continuing study of this class of compounds, we have examined this resonance effect in greater detail and report here the information it provides about the electronic nature of these complexes.

Experimental Section

Crystalline samples of $K_4Ru_2OCl_{10}$, $Cs_4Ru_2OBr_{10}$, and $(NH_4)_4[Os_2OCl_{10}]$ were prepared by previously described procedures.[3]

Raman spectra were determined on a Cary Model 82 spectrometer equipped with a triple monochromator and a krypton and an argon (Coherent Model 52) ion laser. Ultraviolet and visible spectra were determined on a Cary Model 14 spectrophotometer.

Solution Raman spectra were determined on freshly prepared, dilute samples in concentrations ranging from 2×10^{-4} to 5×10^{-3} M. The solubilities of several of the complexes was insufficient in the solvent of choice (5, 6, and 12 M HX) to permit the determination of their spectra. In these instances, the desired solubility was obtained by addition of 18-crown-6 ether. Spectra were determined using a rotating cell.[4a] Raman intensities were determined by adding a known amount of internal standard to the solution and comparing the intensity of the band of interest to that of the $\nu_1(A_1)$ line of the internal standard. At least three spectral scans were made for each determination and the peak areas were measured directly with a polar planimeter. The resulting intensity ratios were averaged, converted to a molar basis, and corrected for phototube response.

Solid-state Raman spectra were obtained with the aid of a rotating cell.[4b] Intensities were determined by adding a known amount of an internal standard such as KNO_3 to the desired μ-oxo-decahalo complex and homogenizing the mixture in a Spex Wig-L-Bug. Integration and normalization procedures were the same as those described for solution samples.

Tetrapotassium μ-oxo-decachloroditungsten(IV) was prepared by a modification of a procedure reported by Colton and Rose.[5] Tungstic acid, H_2WO_4 (12.5 g, 50.0 mmol), was added slowly with stirring to a warm (~75 °C) solution of potassium carbonate (7.5 g) in water (20 ml). The resulting slurry was filtered hot and the filtrate was diluted with water to a total volume of 30 ml. This solution was then added slowly with stirring to 300 ml of boiling concentrated hydrochloric acid. The resulting solution was cooled in an ice bath to ~18 °C and filtered, and the filtrate was treated (in ~1 g portions) with granular (325 mesh) tin (a total of ~8.5 g). Upon the sudden appearance of a deep violet color (~15–20 min from the time addition began), the solution was rapidly gravity filtered through a plug of glass wool into a cooled (0 °C) three-necked, 500-ml, round-bottom flask and the filtrate was saturated with HCl gas. After ~40 min, a crystalline material was observed and collected by suction filtration on a fritted glass funnel. The dark-green crystals, which occasionally appeared as an amorphous magenta powder when precipitated too rapidly, were washed with two 15-ml portions of cold (0 °C) absolute ethanol followed by three 10-ml portions of diethyl ether before drying in vacuo. The isolated yield was 2.2 g (10%). Anal. Calcd. for $K_4W_2OCl_{10}$: K, 17.48; Cl, 39.63; W, 41.10. Found: K, 16.91; Cl, 40.07; W, 39.84; Sn, <0.01.

Results

$Ru_2OX_{10}^{4-}$. The solution electronic spectra of the ions $Ru_2OCl_{10}^{4-}$ and $Ru_2OBr_{10}^{4-}$ are seen in Figures 1 and 2 and tabulated in Table I. They are, in general, poorly resolved, complex spectra. They reveal several parallel features that are noteworthy. Specifically, both spectra reveal a single, moderately intense band between 450 and 500 nm: $Ru_2OCl_{10}^{4-}$ (479 nm, ϵ 5200), $Ru_2OBr_{10}^{4-}$ (492 mn, ϵ 4900). Additional bands appear at higher energies in the spectra of both

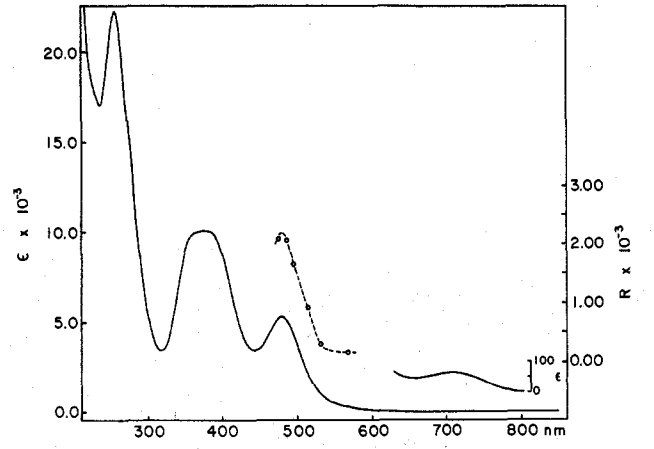

Figure 1. A comparison of the visible absorption spectrum of $K_4Ru_2OCl_{10}$ and the relative intensities (O) of the symmetric Ru–O–Ru stretching vibration. Both Raman and absorption spectra were recorded in 6 M HCl solution. R_{mol} is the molar intensity of the ν(Ru–O–Ru) band divided by the molar intensity of the 1048-cm^{-1} (ν_1) band of KNO_3 added as an internal standard.

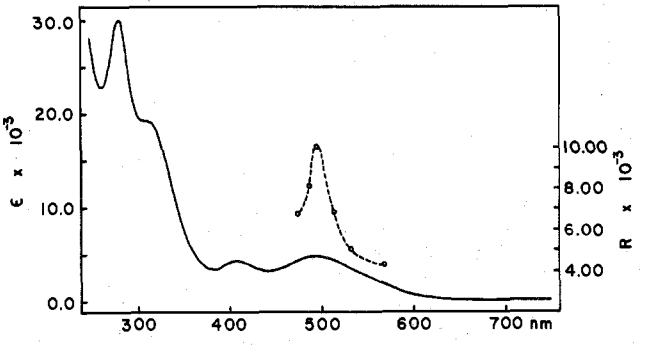

Figure 2. An excitation profile illustrating the influence which exciting frequency has on the relative intensity of the symmetric Ru–O–Ru stretching vibration of $Cs_4Ru_2OBr_{10}$. Both Raman and absorption spectra were recorded in 5 M HBr. The parameters R_{mol} represent the molar intensity of the ν(Ru–O–Ru) band divided by the molar intensity of the 983-cm^{-1} (ν_1) band of Na_2SO_4, added as an internal standard.

complexes. Thus, the spectrum of $Ru_2OCl_{10}^{4-}$ shows an intense band at 254 nm (ε 22 200) and a less intense, unusally broad envelope with a maximum at 375 nm (ε 10 000). The shape of this absorption suggests that more than one band may lie under it. By comparison, the solution electronic spectrum of $Ru_2OBr_{10}^{4-}$ exhibits an intense band at 279 nm (ε 30 000) and two less intense maxima at 310 nm (ε 19,200) and 406 nm (ε 4300). In addition, the spectrum of $Ru_2OCl_{10}^{4-}$ displays a weak band in the far-visible, 712 nm (ε 60). Despite careful examination, a similar band was not observed in the spectrum of $Ru_2OBr_{10}^{4-}$.

The fact that many μ-oxo-bridged transition metal complexes are unstable in solution is well documented. Indeed, much of the early misunderstanding concerning these complexes can be attributed to the failure to recognize this fact. It follows that caution must be exercised in ascertaining whether any of the observed bands in the solution spectra of μ-oxo-bridged complexes result from decomposition products.

Earlier[6a] as well as more recent[6b] investigations of the stability of $Ru_2OCl_{10}^{4-}$ in aqueous solution suggest three principal categories of reaction: (1) aquation, (2) rearrangement (possibly to a di-μ-oxo-bridged species), and (3) cleavage of the dinuclear unit into monomeric species. They conclude, however, that the latter two processes are relatively slow reactions which take place over a period of many hours in aqueous hydrochloric acid (>3 M) at ambient temperatures.

Table I. Electronic Spectra of Some μ-Oxo-Decahalo Species

Complex	λ_{max}, nm	λ_{max}, μm^{-1}	ε, L (mol cm)$^{-1}$
$K_4[Ru_2OCl_{10}]$ in 6 M HCl	712	1.40	60
	479	2.09	5 200
	375	2.67	10 000
	254	3.94	22 200
$Cs_4[Ru_2OBr_{10}]$ in 5 M HBr	492	2.03	4 900
	406	2.46	4 300
	310	3.23	19 200
	279	3.58	30 000
$K_4[W_2OCl_{10}]$ in 12 M HCl sat. with HCl (g)	535 sh	1.87	≳3 800[a]
	300 sh	3.83	4 500
	268 sh	3.73	10 600
	244	4.10	17 200
	230 sh	4.34	16 000
$(NH_4)_4[Os_2OCl_{10}]$ in 5 M HCl	720	1.39	200
	558	1.79	140
	395	2.53	21 500
	332	3.01	12 600
	304	3.29	14 400
	277 sh	3.61	7 900

[a] The intensity of this band decreased rapidly with time. The extrapolated (t = 0) molar absorptivity constant for this band is ~19 000.

They further conclude that the only probable fast reaction that may be occurring is aquation, leading to a mixture of aquo substitution complexes in which the structural integrity of the μ-oxo-bridge is maintained.

Our studies sustain these conclusions. In particular, we observe that solution spectra of $Ru_2OX_{10}^{4-}$ obey the Beer–Lambert law over the concentration range 10^{-4}–10^{-6} M. Moreover, substantially equivalent spectra are observed in aqueous hydrogen halide (6 M) or anhydrous methanol–18-crown-6 solution. Specifically, the principal visible bands at 479 and 492 nm retain their general position and intensity. Taken together, these results exclude an extensive dimer–monomer equilibrium and suggest that the major bands in the electronic spectra shown in Figures 1 and 2 arise from transitions associated with the $Ru_2OX_{10}^{4-}$ ion.

Excitation of a dilute (10^{-3} M) solution of $Ru_2OCl_{10}^{4-}$ with the visible frequencies of either an argon or a krypton laser produces only one readily observable Raman band centered at 254 cm^{-1}. Under equivalent conditions, $Ru_2OBr_{10}^{4-}$ exhibits similar behavior, i.e., a single Raman band at 247 cm^{-1}. We have argued that these bands represent the totally symmetric Ru–O–Ru stretching vibration. Their intensity relative to respectively the 1048 cm^{-1} (ν_1) band of $NaNO_3$ and the 983 cm^{-1} (ν_1) band of Na_2SO_4 (internal standards) was measured at several excitation wavelengths. As seen in Figures 1 and 2, the intensities of the 254-cm^{-1} and of the 247-cm^{-1} band track the 479-nm and 492-nm absorption bands, respectively. We conclude, therefore, that the symmetric Ru–O stretching vibrations in $Ru_2OCl_{10}^{4-}$ and $Ru_2OBr_{10}^{4-}$ are coupled to these respective electronic transitions. It follows that the 479-nm and the 492-nm absorption bands are associated with the metal–oxygen–metal chromophore in $Ru_2OCl_{10}^{4-}$ and $Ru_2OBr_{10}^{4-}$, respectively, and that these transitions must involve significant and presumably parallel changes in the occupancy of the Ru–O–Ru orbitals.

This line of reasoning is further supported by the depolarization studies summarized in Table II. These data show that for both bands, the depolarization ratio remains relatively constant ($\rho_1 \simeq {}^1/_3$) for all near-resonance excitation frequencies. Such behavior is characteristic of a resonance situation in which a single electronic transition enhances a single element of the Raman scattering tensor (e.g., α'_{zz} for a z-polarized elecronic transition).[7] If this element dominates the intensity as anticipated for a totally symmetric vibration such as ν_S(Ru–O–Ru), then the depolarization ratio can be

Table II. The Relative Raman Intensities and Depolarization Ratios for ν_s(M-O-M) in Some Linear μ-Oxo-Decahalo Species

Complex	ν, cm^{-1} Solid	Solution	λ_0[a], Å	ρ[b]	$R_{mol} \times 10^{-3}$ [c] Solid	Solution
$K_4[Ru_2OCl_{10}]$[d]	254	254	4765		1.2	2.1
			4880	0.35	1.6	2.1
			4965		1.9	1.4
			5145	0.34	2.0	0.81
			5309	0.34	1.8	0.28
			5682	0.37	0.34	0.17
			6471		0.24	
$Cs_4[Ru_2OBr_{10}]$[e]	243	247	4765	0.33		6.8
			4880	0.38		8.2
			4965	0.38		10.
			5145	0.37		6.9
			5309	0.34		5.0
			5682	0.34		4.3
			6471			
$K_4[W_2OCl_{10}]$[f]	226	228	4765	0.32	0.25	
			4880	0.38	0.84	
			4965	0.35	1.5	
			5145	0.39	0.98	
			5309	0.37	0.44	
			5682	0.33	0.15	
			6471			
$(NH_4)_4[Os_2OCl_{10}]$[g]	220	230	4765	0.34	1.05	4.56
			4880	0.35	0.825	2.74
			4965	0.32	0.645	1.61
			5145	0.34	0.554	0.662
			5309	0.32	0.607	0.497
			5682	0.37	0.646	0.187
			6471	0.04	0.120	

[a] Exciting wavelength. [b] Depolarization ratio for linearly polarized light. [c] Molar intensity of the ν(M-O-M) band, relative to the ν_1 band of the designated internal standard. $R_{mol} = I_2M_1/I_1M_2$; I = intensity, M = molarity, (solution), mole fraction (solid); 1 = internal standard, 2 = $M_2OX_{10}^{4-}$. [d] Depolarization ratios and solution molar intensities were determined on fresh solutions prepared by dissolving a known amount of $K_4Ru_2OCl_{10}$ in a 4:1 (v/v) mixture of aqueous 6 M HCl-MeOH. Complete dissolution of $K_4Ru_2OCl_{10}$ under these conditions was aided by addition of the cyclic polyether-18-crown-6 (0.22 M). [h] Both solution and solid-state intensities were measured relative to the 1048 cm^{-1} (A_{1g}) band of NO_3^-, added as an internal standard. [e] Solution studies were carried out on freshly prepared solutions of $Cs_4Ru_2OBr_{10}$ in aqueous 5 M HBr. Molar intensity ratios were determined relative to the 983 cm^{-1} (A_{1g}) band of SO_4^{2-}, added as Na_2SO_4. [f] Depolarization ratios were performed on solutions freshly prepared in 12 M HCl. Solid-state molar intensity ratios were determined relative to the 1062-cm^{-1} (A_{1g}) band of anhydrous K_2CO_3. [g] Depolarization ratios were determined in 5 M HCl. Solid-state molar intensity ratios were obtained relative to the 1048-cm^{-1} band of KNO_3. Solution molar intensity studies were carried out in 5 M HCl, relative to the 983-cm^{-1} band of SO_4^{2-} (as Na_2SO_4). [h] G. W. Gokel, D. J. Cram, C. L. Liotta, H. P. Harris, and F. L. Cook, *J. Org. Chem.*, 39, 2445 (1974).

shown to approach $^1/_3$ at resonance.[8]

Finally, it should be noted that the maximum in the excitation profile of $K_4Ru_2OCl_{10}$ obtained from solid-state Raman data falls at ~505 nm. The difference between this value and that observed for solution data (~479 nm) is presumably a result of solid-state effects on the electronic spectrum of this material. This conclusion is sustained by the fact that the reflectance spectrum of $K_4Ru_2OCl_{10}$ (obtained as a 0.1% dispersion in KCl) exhibits three ill-defined bands centered at approximately 420, 375, and 490 nm (in order of decreasing intensity) (cf. Table I). Parallel discrepancies between solution and solid-state resonance Raman intensity data have been observed by other investigators and attributed to similar origins.[9,10]

$W_2OCl_{10}^{4-}$. We have presented evidence,[3] sustained by single-crystal x-ray diffraction,[11] that the dark-green, microcrystalline solid or the magenta-red powder isolated from

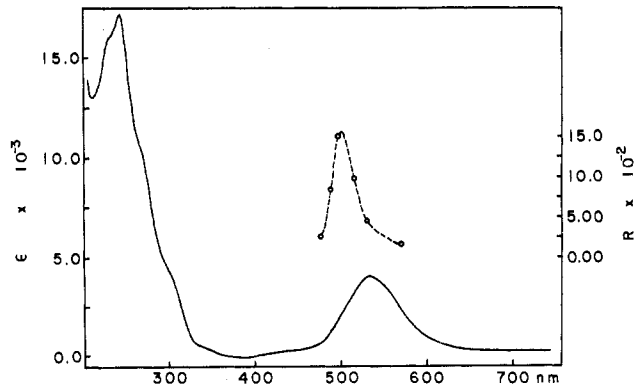

Figure 3. A comparison of the visible absorption spectrum of $K_4W_2OCl_{10}$ (recorded in 12 M HCl) and the relative intensities (O) of ν_s(W-O-W) Raman band recorded on a microcrystalline sample of freshly prepared $K_4W_2OCl_{10}$. The parameter R_{mol} represents the molar intensity of ν_s(W-O-W) band divided by the molar intensity of the 1062-cm^{-1} (ν_1) band of K_2CO_3 added as an internal standard. The intensity of the 535-nm band decreases rapidly with time. The extrapolated (t = 0) molar absorptivity for this band is 19 000.

the incomplete reduction of dipotassium tungstate(VI) by tin in concentrated hydrochloric acid contains the linear μ-oxo-bridged ion $W_2OCl_{10}^{4-}$. The solution electronic spectrum of analytically pure $K_4W_2OCl_{10}$ prepared by an improved procedure (see Experimental Section) and recorded in 12 M HCl is seen in Figure 3. By means of a comparison of disappearance rates of the various major spectral features, we have been able to confirm that the principal band in the optical region (535 nm, ϵ 19 000) arises from a single species, presumably the $W_2OCl_{10}^{4-}$ ion.

The dominant feature in the solid-state Raman spectrum of $K_4W_2OCl_{10}$ is a single intense peak centered at 226 cm^{-1}. In a dilute solution (12 M in HCl) this band appears at 228 cm^{-1}. No other features could be found in solution. We have assigned this band as the symmetric W-O-W stretching vibration. Table II summarizes the influence which changes in excitation frequency have on the solution depolarization ratio of this vibration. They reveal a value of $\rho_1 \simeq {}^1/_3$ for all near-resonance excitation frequencies. The parallel between this result and that observed for $Ru_2OX_{10}^{4-}$ is obvious. It follows that this vibration is coupled to a single resonating electronic transition which enhances a single element of the Raman scattering tensor. Unfortunately, because of the solution instability of $K_4W_2OCl_{10}$, we were unable to obtain meaningful solution Raman intensity data. An excitation profile obtained from solid-state Raman data is shown in Figure 3. The apparent difference between absorption and excitation profile maxima is presumably a reflection of solid-state effects (vide supra) on the electronc spectrum of $K_4W_2OCl_{10}$. We conclude that the Raman band at 228 cm^{-1} and the optical absorption at 535 nm are coupled and that the latter involves a transition of electrons localized in the W-O-W chromophore.

Previous studies[12] have concluded that the $W_2OCl_{10}^{4-}$ ion exists as a mixed valent ion of W(III) and W(V). We have addressed ourselves to this point by examining the information provided by a consideration of the magnetic behavior of $K_4W_2OCl_{10}$. Specifically, we have measured the magnetic susceptibility of $K_4W_2OCl_{10}$ by the Faraday method from 4.2 to 300 K. These results are shown in Figure 4. We have not attempted to fit the data to a detailed model, since an adequate description must include both the tungsten spin–orbit coupling and the C_4 deviation of the crystal field about tungsten from octahedral symmetry. In this case both corrections are expected to be large (~1 eV). Rather, from the measured data we can make some general statements about the electronic (or

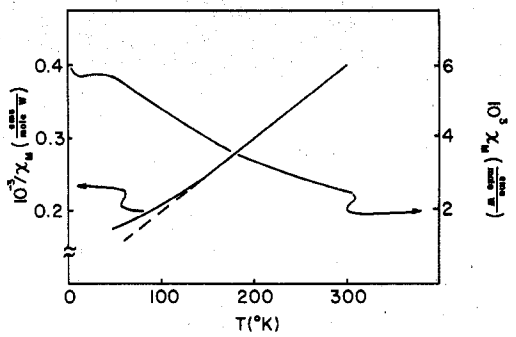

Figure 4. Magnetic susceptibility data for $K_4W_2OCl_{10}$. The susceptibility plot (χ_M vs. T) indicates an antiferromagnetic interaction between tungsten centers. The plot $1/\chi_M$ vs. T provides a Curie–Weiss fit above 150 K (Θ = 97 K) and leads to a calculated value of μ_{eff} = 2.48 μ_B and g = 1.76.

magnetic) levels of the system.

First, in view of the fact that intradimer exchange is expected to be larger by one or two orders of magnitude than interdimer exchange, which typically amounts to only a few degrees,[13,14] it is reasonable to conclude that the interdimer exchange contribution in $K_4W_2OCl_{10}$ can be neglected. It follows that if the tungsten centers in this substance are nonequivalent [e.g., W(V)(d^1) and W(III)(d^3)], the net spin of the dimer at low temperatures would be S = 1 (S = 2) for antiferromagnetic (ferromagnetic) intradimer exchange. It further follows that the susceptibility, under these circumstances, can be expected to increase approximately as $1/T$ at low T.[14] However, as the data in Figure 4 reveal, the measured susceptibility of $K_4W_2OCl_{10}$ below 100 K has only weak temperature dependence. Thus, the two tungsten atoms must be equivalent, i.e., W(IV)(d^2).

Second, additional consideration of these data reveals that at low temperatures the *effective* magnetic moment of the tungsten atoms is zero, since χ is essentially temperature independent. (We neglect the small up turn below 10 K which is most likely due to a very small fraction of impurities.) This result can occur in two ways: (1) the ground state of each tungsten atom is nonmagnetic or (2) the two tungsten atoms in a dimer couple antiferromagnetically. In the former case, the low-temperature susceptibility would be due to a Van Vleck coupling to an excited state Δ K above the ground state. In that case $\chi_M \sim A\mu_B^2/k\Delta$, where A = Avogadro's number leading to $\Delta \sim 60$ K. It would be unusually fortuitous that this small value should result from the normal ordering of individual tungsten states determined by the crystal field and spin–orbit perturbations. For this reason, we discount the first possibility. In the second case, if the tungsten moments were due to spin only the susceptibility would approach zero as $T \rightarrow 0$. However, this is not expected to be an accurate description of the magnetic state since the electron configuration is d^2 and the spin–orbit coupling is large. Again in this case, the magnitude of the susceptibility at low temperatures would be given by $\chi_M \approx A\mu_B^2/k\Delta$, with Δ being the splitting produced by the exchange coupling. Also, it is expected that at high temperatures ($T \gg \Delta$), $\chi_M = A\mu_B^2g^2S(S+1)/3k(T+\Theta)$ (neglecting the small independence correction due to core diamagnetism). Indeed a plot of $1/\chi$ vs. T in Figure 4 is linear above ~150 K. Moreover, this treatment leads to a predicted g value of 1.76 (with S = 1) and $\Theta \approx 100$ K, a value in close agreement with that determined by ESR (1.78).[15] The exchange energy obtained from simple mean field models, i.e., $J = 3\Theta/25(S+1)$, is 75 K.

Thus, we conclude that the magnetic data show that the tungsten centers in $K_4W_2OCl_{10}$ are d^2 and are antiferromagnetically coupled with an exchange energy of ~75 K. The spin–orbit coupling produces a large shift of the g value from 2 to 1.76, and this coupling along with the C_4 crystal field and the intradimer exchange most likely account for the nonzero susceptibility observed at low temperatures by way of Van Vleck coupling to an excited magnetic state.

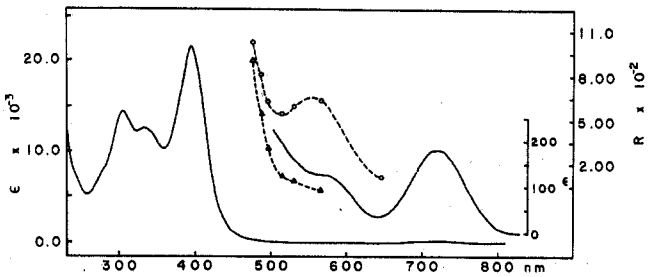

Figure 5. An excitation profile illustrating the influence which exciting frequency has on the relative intensities of the ν_s(Os–O–Os) Raman band. Solution Raman and absorption spectra were recorded in 5 M HCl. The parameter R_{mol} represents the molar intensity of the ν_s(Os–O–Os) band divided by the molar intensity of the 983-cm^{-1} (ν_1) band of Na_2SO_4 added as an internal standard. Solid-state molar intensities are denoted by (○); those determined in solution are designated by (Δ). For plotting purposes, the solution relative intensities (Δ) were obtained by multiplying the observed ratios by a factor of 5.

$Os_2OCl_{10}^{4-}$. Although salts of μ-oxo-decachlorodiosmium(IV) ions are diamagnetic in the solid state, in aqueous solution these substances exhibit temperature- and concentration-dependent paramagnetism.[16] This significant difference between the solid-state and solution nature of $Os_2OCl_{10}^{4-}$ has been interpreted as indicating that extensive dissociation of the diamagnetic dimer into a paramagnetic monomer occurs in solution.[16] The comparative complexity of the solution electronic spectrum of $Os_2OCl_{10}^{4-}$ (cf. $Ru_2OCl_{10}^{4-}$) is presumably a reflection of this behavior. Thus, the electronic spectrum of $(NH_4)_4Os_2OCl_{10}$ in 6 M HCl solution is characterized by three intense, rather closely spaced, high-energy bands: 304 nm (ε 14 400), 332 nm (ε 12 600), and 395 nm (ε 21 500). What may be a fourth band appears as a shoulder at 277 nm on the 304-nm band. In addition there are also two broad bands of considerably reduced intensity with maxima at 558 nm (ε 140) and 720 nm (ε 200) (Figure 5).[17]

The Raman spectrum of $(NH_4)_4Os_2OCl_{10}$ is dominated by a single intense band centered at 220 cm^{-1} in the solid state and 230 cm^{-1} in dilute solution (6 M in HCl). We have argued that this band corresponds to the totally symmetric (A_{1g}) Os–O–Os stretching vibration.[3] Figure 5 shows the variation in the relative intensity of this band with excitation frequency as observed for both solid-state and solution Raman spectra. A comparison of these two profiles reveals a prominent difference: the intensity of the 220-cm^{-1} (solid-state) band tracks the 558-nm electronic absorption and then continues to rise as the excitation wavelength approaches the 395-nm band, while the intensity of the 230-cm^{-1} (solution) band follows only the 395-nm absorption. One interpretation of these results is that in the solid state ν_S(Os–O–Os) is in resonance with both the 558-nm and the 395-nm band, but that in solution the intensity of the 558-nm absorption is so diminished as a result of dimer dissociation that resonance with the more intense 395-nm band becomes dominant.[18] An alternative explanation which cannot be dismissed under the present circumstances is that the 230-cm^{-1} band arises from a decomposition product. Regardless of which explanation is correct, it nonetheless follows that the 558-nm band is associated with the μ-oxo-bridged unit in $Os_2OCl_{10}^{4-}$.

The correspondence between the maximum in the solid-state excitation profile and the maximum in the solution optical spectrum of $Os_2OCl_{10}^{4-}$ (558 nm) parallels the behavior observed for $Ru_2OCl_{10}^{4-}$, $Ru_2OBr_{10}^{4-}$, and $W_2OCl_{10}^{4-}$ and

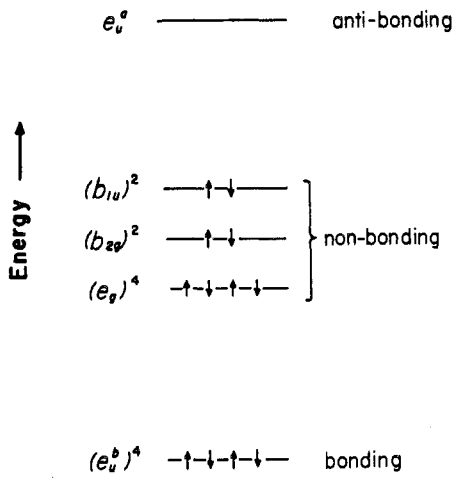

Figure 6. Diagram showing the relative energies of the π component of the molecular orbital scheme for $Ru_2OX_{10}^{4-}$ and $Os_2OX_{10}^{4-}$. The nonbonding e_g, b_{2g}, and b_{1u} orbitals are closely spaced with an arbitrary sequence that is not meant to imply a specific ordering. By removing respectively two (2) and four (4) electrons from the nonbonding level, a corresponding description of the π bonding in $Re_2OX_{10}^{4-}$ and $W_2OCl_{10}^{4-}$ is generated.

suggests the possibility that all these transitions may have similar origins. The gradual red shift in position of this band in proceeding from $Ru_2OCl_{10}^{4-}$ (479 nm) to $Ru_2OBr_{10}^{4-}$ (492 nm) to $W_2OCl_{10}^{4-}$ (535 nm) to $Os_2OCl_{10}^{4-}$ (558 nm) is also consistent with the anticipated decrease in separation between ground and excited electronic states that generally occurs in the electronic spectra of transition metal complexes of similar molecular orbital arrangement when proceeding from second- to third-row metals.[19]

Discussion

Dunitz and Orgel[20,21] have presented a plausible molecular orbital treatment of the bonding in the $Ru_2OCl_{10}^{4-}$ ion which explains its unusual features, i.e., diamagnetism, short Ru–O bond length and the linear geometry of the Ru–O–Ru group. The resulting ground state configuration (exclusive of σ components)[22] is described by $(e_u^b)^4\,[(b_{2g})^2(b_{1u})^2(e_g)^4]\,(e_u^a)^0$, in which the orbitals in square brackets are approximately degenerate and nonbonding and the e_u^b and e_u^a orbitals describe respectively a set of bonding and antibonding orbitals. This same description can be extended to explain the bonding in $Os_2OCl_{10}^{4-}$, which is both isostructural and isoelectronic with $Ru_2OX_{10}^{4-}$, as well as the $Re_2OCl_{10}^{4-}$ and $W_2OCl_{10}^{4-}$ ions which, although isostructural with $Ru_2OX_{10}^{4-}$, involve electronically dissimilar metals (cf. Figure 6).

It can be anticipated that a M–O–M stretching mode will be strongly enhanced by resonance involving a transition between a bonding or nonbonding orbital and an antibonding orbital. Assignment of such a transition as largely d–d is unlikely for this reason. In the present molecular orbital framework, the likeliest transitions are $e_u^b \rightarrow e_u^a$, $b_{2g} \rightarrow e_u^a$, $b_{1u} \rightarrow e_u^a$, and $e_g \rightarrow e_u^a$.[20] Two of these, $e_u^b \rightarrow e_u^a$ and $b_{1u} \rightarrow e_u^a$, can be immediately dismissed because they involve electric dipole forbidden processes. Of the remaining two processes, only one ($e_g \rightarrow e_u^a$) is expected to have any significant intensity.[23] Therefore, we conclude that the totally symmetric M–O–M stretching vibration in $Ru_2OX_{10}^{4-}$, $W_2OCl_{10}^{4-}$, and $Os_2OCl_{10}^{4-}$ is in resonance with a single electronic transition which, within the framework of the Dunitz–Orgel molecular orbital description, corresponds to the promotion of an electron from a nonbonding e_g to antibonding e_u^a orbitals ($^1A_{1g} \rightarrow {}^1A_{2u}$ in molecular symmetry notation) corresponding to a transition from a nonbonding π to π^*. Since this transition is z polarized,[23] it follows that α'_{zz} is the dominant element in the Raman scattering tensor of the M–O–M vibration that is enhanced by resonance.

The above results provide convincing evidence that the bonding in the μ-oxo-bridged complexes, in contrast to certain other systems (vide infra), can be usefully described by a molecular orbital description. Regardless of the bonding scheme employed, one conclusion remains inescapable: the electronic transition observed in the optical spectra of $Ru_2OX_{10}^{4-}$, $Os_2OCl_{10}^{4-}$, and $W_2OCl_{10}^{4-}$ and characterized by its resonant coupling with ν_S(M–O–M) involves electrons spanning the M–O–M group and establishes the M–O–M unit as an electronically unique and independent chromophore.

A cautionary note is appropriate at this point. The unqualified extension of these results to linear μ-oxo-bridged complexes in general is unwarranted. Lest this statement seem gratuitous, consider the following two examples. The structure of the binuclear anion μ-oxo-bis[oxotetracyanorhenium(V)], $[ORe(CN)_4ORe(CN)_4O]^{4-}$, has been established by a single-crystal x-ray diffraction study as containing a linear O=ReORe=O grouping with the cyanide ligands completing the octahedral environment about each rhenium.[24] The electronic spectrum of $K_4[Re_2O_3(CN)_8]$ (recorded in aqueous solution) is characterized by two absorptons [300 nm (ϵ 31 200) and 540 nm (ϵ 273)];[25] the latter band is responsible for the intense purple color of the $Re_2O_3(CN)_8^{4-}$ ion in both the solid state and in solution. Both bands remain unassigned. An examination of the Raman spectrum of this material over a range of excitation frequencies using plasma lines (5145 and 5309 Å) which lie particularly close to the maximum of the low-energy visible absorption failed to reveal any band of significant intensity in the low-energy region (<400 cm^{-1}). Indeed, the dominant, and essentially the only feature in the Raman spectrum of $K_4Re_2O_3(CN)_8$ below 1000 cm^{-1} is a band at 980 cm^{-1} which we assign as ν(Re=O).

A second example is the compound $enH_2[(FeHEDTA)_2O]\cdot 6H_2O$ which contains a near-linear (165°) Fe–O–Fe unit.[26] It has been argued, based on the results of an extensive study of the electronic spectra and magnetic susceptibility data for this compound, that its electronic structure is more accurately described by a simple high-spin ligand-field model rather than by a Dunitz–Orgel molecular orbital approach.[27] Accordingly, the several bands that appear in the visible spectrum of this complex were assigned as one-center Fe(III) ligand-field transitions. The fact that the Raman spectrum of this substance shows very little variation with changes in excitation frequency and revealed no prominent band below 400 cm^{-1} which could be readily assigned as ν_S(FeOFe) is consistent with (but does not require) this conclusion.

These observations serve to underline the fact that, in the absence of electronic homogeneity, structural similarities between compounds will not necessarily be revealed by a comparison of their Raman spectra, and, in general, functional group analysis by Raman spectroscopy must be accompanied by a consideration of the electronic nature of the compound under investigation.

Acknowledgment. We are deeply indebted to Professor Lionel Goodman of this department for many extremely helpful discussions during the course of this work.

Registry No. $K_4[Ru_2OCl_{10}]$, 16986-07-5; $Cs_4[Ru_2OBr_{10}]$, 57304-87-7; $K_4[W_2OCl_{10}]$, 19644-53-2; $(NH_4)_4[Os_2OCl_{10}]$, 22827-22-1.

References and Notes

(1) (a) Rutgers University, with support by the National Institutes of Health (AM-18713-01) and by the Petroleum Research Fund, administered by the American Chemical Society; (b) Bell Laboratories.
(2) S. B. Brown, P. Jones, and I. R. Lantzke, *Nature (London)*, **223**, 960 (1969); M. Y. Okamura, I. M. Klotz, C. E. Johnson, M. R. C. Winter, and R. J. P. Williams, *Biochemistry*, **8**, 1951 (1969); J. L. York and A. J. Bearden, *ibid.*, **9**, 9549 (1970); T. H. Moss, C. Moleski, and J.

L. York, *ibid.*, **10**, 840 (1971); H. B. Gray, *Adv. Chem. Ser.*, No. **100**, 365 (1971); J. W. Dawson et al., *Biochemistry*, **11**, 461 (1972).
(3) J. San Filippo, Jr., R. L. Grayson, and H. J. Sniadoch, *Inorg. Chem.*, **15**, 269 (1976).
(4) (a) W. Kiefer and H. J. Bernstein, *Appl. Spectrosc.*, **25**, 500 (1971); (b) *ibid.*, **25**, 609 (1971).
(5) R. Colton and G. G. Rose, *Aust. J. Chem.*, **21**, 883 (1968).
(6) (a) J. L. Woodhead and J. H. Fletcher, A.E.R.E. Report, 4123 (Hartwell), England, 1962; (b) I. P. Alimarin, V. I. Shlenskaya, and Z. A. Kuratashvili, *Russ. J. Inorg. Chem.* (*Engl. Transl.*), **18**, 250 (1973).
(7) R. E. Hester, "Raman Spectroscopy", H. A. Symanski, Ed., Plenum Press, New York, N.Y., 1967, Chapter 4.
(8) The molecular symmetry of the $M_2OX_{10}^{4-}$ ion is D_{4h}. In this point group the totally symmetric vibrations (A_{1g}) have scattering tensors with diagonal elements only: α'_{xx}, α'_{yy}, α'_{zz}. Under such circumstances the depolarization ratio can be shown[7] to have the form

$$\rho_1 = {}^1/_3 \frac{(\alpha'_{xx})^2 + (\alpha'_{yy})^2 + (\alpha'_{zz})^2 - \alpha'_{xx}\alpha_{yy} - \alpha'_{xx}\alpha'_{zz} - \alpha'_{yy}\alpha'_{zz}}{(\alpha'_{xx})^2 + (\alpha'_{yy})^2 + (\alpha'_{zz})^2 + {}^2/_3\alpha'_{xx}\alpha'_{yy} + {}^2/_3\alpha'_{xx}\alpha'_{zz} + {}^2/_3\alpha'_{yy}\alpha'_{zz}}$$

When one element is dominant, this reduces to $\rho_1 \simeq {}^1/_3$.
(9) R. S. Chao, R. K. Khanna, and E. R. Lippincott, *J. Raman Spectrosc.*, **3**, 121 (1975).
(10) It has been suggested[9] that when discussing solid-state resonance Raman data, it may actually be preferable to employ the maximum in the excitation profile determined from solid-state Raman intensity data as the effective electronic frequency, ν_e, rather than the value traditionally obtained from the solution UV-vis spectrum.
(11) Following the completion of our earlier study (ref 3) an investigation detailing the crystal structure of $K_4W_2OCl_{10}$ and its isostructural relationship to $K_4Re_2OCl_{10}$, $K_4Ru_2OCl_{10}$, and $Cs_4Os_2OCl_{10}$ appeared: T. Glowiak, M. Sabat, and B. Jezowska-Trzebiatowska, *Acta Crystallogr., Sect. B*, **31**, 1783 (1975).
(12) E. König, *Inorg. Chem.*, **8**, 1278 (1969).
(13) M. E. Lines, A. P. Ginsberg, and F. J. Di Salvo, *J. Chem. Phys.*, **61**, 2095 (1974).
(14) A. P. Ginsberg, *Inorg. Chim. Acta, Rev.*, **5**, 45 (1971).
(15) At 110 K the g value for solid $K_4W_2OCl_{10}$ as determined by ESR is 1.778. A similar value (g = 1.76 at 25 °C) was previously reported by R. Colton and G. G. Rose, *Aust. J. Chem.*, **21**, 883 (1968).
(16) B. Jezowska-Trzebiatowska, J. Hanuza, and W. Wojciechowski, *J. Inorg. Nucl. Chem.*, **28**, 2701 (1966).
(17) These observations compare favorably with the solution absorption spectrum of $(NH_4)_4[Os_2OCl_{10}]$ reported in ref 16. In addition, these authors also report the appearance of a broad band in the near-IR region, centered at 1050 nm (ϵ 240).
(18) The reflectance spectrum of $(NH_4)_4Os_2OCl_{10}$ was too diffuse and ill-defined to permit a meaningful comparison to the solution spectrum.
(19) J. San Filippo, Jr., *Inorg. Chem.*, **11**, 3140 (1972).
(20) J. D. Dunitz and L. E. Orgel, *J. Chem. Soc.*, 2594 (1953).
(21) See also W. Klemm and K. H. Raddatz, *Z. Anorg. Allg. Chem.*, **250**, 207 (1942); B. N. Figgis and J. Lewis, *Prog. Inorg. Chem.*, **6**, 148 (1964).
(22) Transitions involving electrons from the σ framework are likely to occur at much higher energies than the resonating electronic transition observed in the present study and for this reason are not considered in the present discussion.
(23) This statement follows from a consideration of the magnitude of the transition dipole moment, μ, in the approximate expansion of the relevant MO in terms of atomic orbitals localized on M_1, M_2, and O.

$$\mu_{e_g \rightarrow e_u{}^a} = \langle d_{xz}(M_1)\mu d_{xz}(M_1)\rangle - \langle d_{xz}(M_2)\mu d_{xz}(M_2)\rangle - \langle d_{xz}(M_2)\mu \underset{y}{p_x}(O)\rangle + \langle d_{xz}(M_2)\mu \underset{y}{p_x}(O)\rangle = -2\langle d_{xz}(M_2)\mu d_{xz}(M_2)\rangle$$

which reduces to $\mu_{e_g \rightarrow e_u{}^a} = -2\mathbf{R}_{M\text{-}O}$, where $\mathbf{R}_{M\text{-}O}$ is the length of the metal oxygen bond. However, at the same level of approximation

$$\mu_{b_{2g}} \rightarrow e_u{}^a = \langle d_{xy}(M_1)\mu \underset{yz}{d_{xz}}(M_1)\rangle + \langle d_{xy}(M_2)\mu \underset{yz}{d_{xz}}(M_2)\rangle - \langle d_{xy}(M_1)\mu \underset{y}{p_x}(O)\rangle - \langle d_{xy}(M_2)\mu \underset{y}{p_x}(O)\rangle = 0$$

We conclude, therefore, that only the $e_g \rightarrow e_u{}^a$ transition can be expected to have an appreciable intensity. Moreover, it can be shown by local symmetry arguments that this transition will have z polarization.
(24) R. Shandles, E. O. Schlemper, and R. K. Murmann, *Inorg. Chem.*, **10**, 2785 (1971).
(25) D. L. Toppen and R. K. Murmann, *Inorg. Nucl. Chem. Lett.*, **6**, 139 (1970).
(26) S. J. Lippard, H. J. Schugar, and C. Walling, *Inorg. Chem.*, **6**, 1825 (1967).
(27) H. J. Schugar, G. R. Rossman, C. G. Barraclough, and H. B. Gray, *J. Am. Chem. Soc.*, **94**, 2683 (1972).

Contribution from the Materials and Molecular Research Division, Lawrence Berkeley Laboratory, Berkeley, California 94720, and the Chemistry Division, Atomic Energy Research Establishment, Harwell, England

Spectral Properties of $(Et_4N)_2UI_6$ and $(Et_4N)_2UF_6$

W. WAGNER,[1a] N. EDELSTEIN,*[1a] B. WHITTAKER,[1b] and D. BROWN*[1b]

Received November 23, 1976 AIC60845T

The optical spectra of $(NEt_4)_2UI_6$ and $(NEt_4)_2UF_6$ are presented and analyzed. With these data the electrostatic, spin–orbit, and crystalline field parameters have been obtained for the series of octahedral compounds UX_6^{2-} (X = F, Cl, Br, I). The Slater parameter F^2 diminishes approximately 20% as the halide ion changes from F^- to I^-. The crystalline (or ligand) field parameters for comparable PaX_6^{2-} and UX_6^{2-} compounds vary markedly.

Introduction

The preparation and spectral properties of octahedral compounds of the type $(NEt_4)_2PaX_6$ (X = F, Cl, Br, I) have recently been investigated.[2,3] The trends in the ligand field parameters θ and Δ for these $5f^1$ complexes were explained qualitatively in terms of molecular orbital theory by large variations in σ bonding dominating the total ligand field splitting and changing markedly as the halide ion varied. This same trend was also found for salts of the hexahalogenouranates (V). As part of the above program the corresponding $(NEt_4)_2UX_6$ (X = F, Cl, Br, I) salts were prepared and their optical spectra obtained at 77 K.[2b,3] The most thorough analyses of the octahedral UX_6^{2-} spectra (X = Cl, Br) have been given by Satten and co-workers from data obtained at 4 K on U^{4+} diluted in single crystals.[4-6] We report in this paper the analyses of the spectra of $(NEt_4)_2UX_6$ (X = I, F) and compare the trends in the parameters obtained for the U^{4+} series ($5f^2$) as the halide ion is varied, with the corresponding parameters in the $5f^1$ series.

Experimental Section and Calculations

The preparation of $(NEt_4)_2UI_6$ and $(NEt_4)_2UF_6$ and the recording of their spectra at room temperature and 77 K have been described previously.[2,3,7]

Calculated energies were obtained by the simultaneous diagonalization of the combined electrostatic, spin–orbit, and crystalline field matrices which were constructed by the tensor operator methods described by Judd[8] and Wybourne.[9] These matrices were factored by the crystal quantum number, μ, into a 25 × 25 matrix (μ = 0, Γ_1 and Γ_2 states), a 24 × 24 matrix (μ = 2, Γ_3 and Γ_4 states), and two 21 × 21 matrices (μ = 1, a doubly degenerate Γ_5 state). Matrices of these ranks can be easily diagonalized by existing computer programs so no further factoring was necessary. Experimental energies were compared with calculated energies and the parameters of the